Combination of geophysical and geotechnical data using belief functions: Assessment with numerical and laboratory data

Théo Dezert, Sérgio Palma Lopes, Yannick Fargier, Philippe Côte

Combination of geophysical and geotechnical data using belief functions: assessment with numerical and laboratory data

T. Dezert[a,b], S. Palma Lopes[a], Y. Fargier[b,c] P. Côte[a]

[a] IFSTTAR, GERS, GeoEND, F-44344 Bouguenais, FRANCE, theo.dezert@ifsttar.fr, sergio.lopes@ifsttar.fr, philippe.cote@ifsttar.fr
[b] Cerema Direction territoriale Normandie-Centre, F-41000 Blois, FRANCE
[c] Univ Lyon, IFSTTAR, GERS, RRO, F-69675 Bron, FRANCE, yannick.fargier@ifsttar.fr

Declarations of interest: none.

Abstract

The identification of the subsoil constitutive materials, as well as the detection of possible interfaces and anomalies, are crucial for many site characterization applications. During investigation campaigns, complementary geophysical and geotechnical methods are usually used. These two sets of methods yield data with very different spatial scales and different levels of incompleteness, uncertainty and inaccuracy. In this work, a mathematical combination of geophysical and geotechnical information is proposed in order to produce a better subsoil characterization. It is shown that belief functions can be used for such a fusion process. A specific methodology is developed in order to manage conflictual information and different levels of uncertainties and inaccuracies from different investigation methods. In order to test and validate this methodology, we focus on the use of two selected methods, Electrical Resistivity Tomography (ERT) and Cone Penetration Test. First, a synthetic model with artificial data is considered, taking advantage of the results obtained to conduct a comparative study (effect of parameters and noise level). Then, an experimental test bench is considered, in which a two-layered model is placed (plaster and saturated sands) and geophysical and geotechnical data are generated, using a mini-ERT device and insertion depth values. This work also aims at providing a better graphical representation of a subsoil section with associated degrees of belief. The results highlight the ability of this fusion methodology to correctly characterize the considered materials as well as to specify the positions of the interfaces (both vertical and horizontal) and the associated levels of confidence.

Key Words

Data fusion, belief functions, geophysical data, geotechnical data, experimental test bench, electrical resistivity tomography.

I. Introduction

For subsoils characterization, investigation campaigns are set up, usually consisting of geophysical and geotechnical methods. These two families of methods are complementary and are used for various issues such as the characterization of slope stability [1-4] the characterization of potentially dangerous sites [5], the characterization of sites at construction [6] or the characterization of river embankments [7].

On the one hand, geophysical methods are non-intrusive and provide physical information on large volumes of soils but with significant potential uncertainties. These uncertainties are due in particular to the integrative and indirect aspects of the methods as well as to the resolution of the inverse problems. On the other hand, the geotechnical investigation methods are intrusive and provide more punctual information but also more accurate. An important issue for the assessment of subsoils is to be able to combine acquired geophysical and geotechnical data, while taking into account their respective uncertainties, inaccuracies and spatial distributions [8]. The complementarity of these two sets of methods is often underused since the uncertainty and inaccuracy associated with each method are rarely considered. Furthermore, the results are usually only graphically superimposed [9] instead of being mathematically merged.

To characterize a section of subsoil and its potentially risky areas, it is essential to distinguish the different materials in place. The horizontal and vertical interfaces, as well as possible anomalies, have to be located. For levee embankment, as an example, it is in these locations that internal erosion is likely to develop, which

may lead to the complete rupture of the levee [10]. Such a section characterization, with associated confidence indexes, could be included in failure hazard models.

The use of belief functions [11-12] and different information combination rules to combine geotechnical and geophysical data is proposed. This makes it possible to take into account at the same time the uncertainties, inaccuracies and incompleteness of data related to each method. In the field of geosciences, belief functions have already been used and provide interesting results for slope instability mapping [13-14], detection of precious metal [15], groundwater [16] or flood susceptibility mapping [17]. To our best knowledge, no work has been proposed, considering the combination of two sources of information with different spatial distribution (spatialized and punctual) and for an investigation campaign in the vertical section.

Here, an innovative method of information fusion to combine electrical resistivity tomography results and cone penetrometer test data is proposed. First, work on data obtained from synthetic models is displayed. The obtained results allow to conduct a comparative study, evaluating the effect of different parameters (like the data noise level) on the fusion result. The fusion methodology is then tested from data acquired on a test bench. In this work, the potential of such a methodology is shown by using insertion depth data, acquired by a laboratory penetration cone, and electrical resistivity data acquired by a mini Electrical Resistivity Tomography (ERT) device. The depth of penetration data corresponds to geotechnical information while the electrical resistivity data correspond to geophysical information. The main concern is to highlight the ability of this information fusion algorithm to characterize the interfaces between materials and to discriminate three different types of materials with variation in thickness of one of them, and to present the variation of the results according to the number and position of the simulated boreholes.

The main contributions of this work are as follows. First, this new methodology makes it possible to take into account the uncertainties, inaccuracies and incompleteness associated with the different methods of investigation used, proposing a modeling of the Basic Belief Assignments (BBAs) specifically adapted to the problematic. Then, the proposed graphic representation is innovative since it allows both to present the different geological sets that would be present in the subsoil and their layout, while presenting the confidence associated with these results. This methodology is particularly suitable for the characterization of interfaces and anomalous zones, which may correspond to areas where the risk of instability is potentially the greatest. This work also allows the implementation of a small physical model to validate the fusion approach with real data.

This article is organized as follows. In section II a presentation of the approach of fusion used in the methodology is given, which introduces the use of the evidence theory and the combination methods used here. In section III, a synthetic study will then present the fusion approach from artificial data. It will also present the comparative results associated to two parametric studies. Then, in section IV, a presentation of the investigation methods used in the introduced experiment (laboratory penetration cone and mini ERT device) is given. Finally, the test bench fusion results are presented in section V and discussed in section VI, in order to understand the interests, limitations and perspectives of such a methodology.

II. Fusion methodology

1) Belief functions and combination rules

The belief functions have been introduced by Shafer [11] in 1976 in the development of his mathematical theory of evidence inspired by previous works of Dempster [12]. Shafer's theory is also referred as Dempster-Shafer theory (DST) in the literature. This theory (proposes a method to) calculate(s) the belief and the plausibility of an event (here a soil material class) from distinct source of evidence (measured data). The practical advantage of using such a theory lies in its ability to manage information from different sources, associated with variable uncertainties and inaccuracies. In this work, only two sources of information will be considered: geotechnical and geophysical. Another advantage of this theory is its ability to assess the degree of conflict between sources (ex: contradictory information between data obtained from large scale geophysical campaign and from punctual geotechnical investigation). Uncertainties correspond to degrees of confidence that are given to a value, whereas inaccuracies correspond to intervals of values that can be directly associated with measurement errors related to the method. For example, the uncertainty of measuring a geotechnical parameter identical to the one measured in a borehole increases with the distance to that point. The inaccuracy can for its part, be associated with the error bar of the result. The belief functions allow to take into account the ignorance and incompleteness of the information. It is indeed possible to grant credit on

all the possible results in order to quantify the ignorance. For the reader eager to learn more, the theory is detailed in [18].

A Bayesian approach as part of a subjective probability approach [19] could have been considered for geophysical and geotechnical data combination. However, the main limitation of such an approach is that probabilities essentially represent uncertainty and only very poorly the level of inaccuracy. Moreover, in the probabilistic modeling stage, the different decisions (events) are only represented on singletons (i.e. single events) and are necessarily considered exhaustive and exclusive. The exclusivity is implied by the assumption of the additivity of probabilities. However, this hypothesis may be too strong and limit the representation of the knowledge. Furthermore, with a Bayesian approach, it is difficult to model the lack of knowledge or the knowledge that is not expressed in probability distributions.

In order to define and to use the belief functions, it is necessary (i) to set a frame of discernment, (ii) to assign belief mass values to the events of this framework (Basic Belief Assignments - BBAs), (iii) to choose a fusion rule for combining information; and (iv) to represent the combined information.

The Frame of Discernment Θ (FoD) is made of all the possible events about the problem under concern, the elements of the FoD are exclusive and exhaustive, so that for *n* events:

$$\Theta = \{\theta_1, \theta_2, \dots, \theta_n\} \tag{1}$$

In the considered problematic, the possible events of the FoD correspond to intervals of values of geophysical and geotechnical parameters that can be associated with classes of geological materials (for example, θ_1=clays, θ_2=sands…). The space of belief mass functions, the set of all subsets of Θ, written 2^{Θ}, is fixed by all the disjunctions and by the possible conflict between the sources of information (written $\emptyset$) such that:

$$2^{\Theta} = \{\emptyset, \{\theta_1\}, \{\theta_2\}, \{\theta_1 \cup \theta_2\}, \{\theta_3\}, \{\theta_1 \cup \theta_3\}, \{\theta_2 \cup \theta_3\}, \{\theta_1 \cup \theta_2 \cup \theta_3\}, \dots, \{\theta_1 \cup \theta_2 \cup \theta_3 \cup \dots \cup \theta_n\}\} \tag{2}$$

As in the probability theory, the belief mass function m_j is defined, for a source of evidence S_j (for j=1, 2), attributed to *A* (defined on 2^{θ}) in [0, 1] such that the more *m(A)* tends to 1 and the more the confidence in *A* is important :

$$\sum_{A \epsilon 2^{\Theta}} m_j(A) = 1 \tag{3}$$

The difference with the probability theory lies in the fact that *A* can represent the union of several events (for example, either θ_1 OR θ_2). It is therefore possible to model uncertainty and lack of knowledge. For instance, when no information is available about the achievement of an event member of Θ, one can set $m_j(\Theta) = 1$, avoiding the uniform distribution that would have been considered in a probabilistic scheme. Combination rules, as part of the belief functions theory, can thus take different levels of uncertainty and imprecisions into account according to the source of information. If only defined on singletons, the belief mass function is similar to a probability distribution.

Smets fusion approach developed in his Transferable Belief Model (TBM) [20] (i.e. conjunctive fusion) allows the attribution of a mass of belief to the conflict, outside the FoD, so that (open-world assumption):

$$m_{12}(\emptyset) > 0 \tag{4}$$

Where $m_{12}(\cdot)$ denotes the combined BBA resulting from the combination of information of sources 1 and 2. The belief mass resulting from the fusion of information from source 1 and 2 is written:

$$m_{12}(\mathrm{A}) = \sum_{X,Y \subseteq \Theta | X \cap Y = \mathrm{A}} m_1(X) m_2(Y) \tag{5}$$

And the level of conflict between the two considered sources of information can therefore be quantified by:

$$m_{12}(\emptyset) = \sum_{X,Y \subseteq \Theta | X \cap Y = \emptyset} m_1(X) m_2(Y) \tag{6}$$

With $m_1(X)$ and $m_2(Y)$ the belief masses respectively attributed to events *X* and *Y* by sources *1* and *2*.

According to Shafer's approach and unlike Smets' rule, Dempster-Shafer's rule (DS) does not allow the attribution of a mass of belief to the conflict (closed-world assumption):

$$m_{12}^{DS}(\emptyset) = 0 \tag{7}$$

The conflict is there reallocated through a classical normalization factor. The mass of belief in A, $m_{12}^{DS}(A)$, resulting from the fusion of information from sources 1 and 2 is written:

$$m_{12}^{DS}(A) = \frac{1}{1 - m_{12}(\emptyset)} \sum_{X,Y \subseteq \Theta | X \cap Y = A} m_1(X) m_2(Y) \tag{8}$$

The disadvantage of this method is that the conflict between the sources is no longer represented and it is possible to obtain counterintuitive results if the conflict is important because of this normalization. Even more problematic, even if the distinct sources are both informative whatever the level of conflict is, Dempster-Shafer's fusion process can even not take into account the second source of information [21].

On the other hand, the PCR6 (Proportional Conflict Redistribution No. 6) rule of combination [22-23], considering two sources of information, only transfers the conflicting mass to the events that are actually implied in the conflict and in proportion with their individual masses in order to preserve the specificity of the information. In order to apply the PCR6 rule : i) the combination rule described in Eq (5) must be applied, ii) the total or partial conflicting masses have to be calculated and iii) the total of partial conflicting masses have to be redistributed proportionally on non-empty sets. So, for $m_{12}^{PCR6}(\emptyset) = 0$ and $\forall\ A \in 2^{\Theta} \setminus \{\emptyset\}$:

$$m_{12}^{PCR6}(A) = m_{12}(A) + \sum_{\substack{Y \in 2^{\Theta} \\ A \cap Y = \emptyset}} \left[\frac{m_1(A)^2 m_2(Y)}{m_1(A) + m_2(Y)} + \frac{m_2(A)^2 m_1(Y)}{m_2(A) + m_1(Y)} \right] \tag{9}$$

2) Construction of BBAs from geophysical and geotechnical data

Belief masses have to be assigned to each considered event of the FoD, for both sources of information. The combination of the belief masses can only be initiated after this stage. In the following, the geophysical source of information will be identified as source 1 and the geotechnical source of information as source 2. A 2D model assumption will be made, corresponding to the x and z spatial axes, since vertical sections of subsoil are considered.

Geophysical data

The discretization of the considered subsoil section, as well as the depth of investigation and the resolution, depend on the acquisition method used [24]. It is the user who sets, using the inversion tool used, the shape and dimensions of the discretization grid used. It is about starting from this discretization and being able to associate for each cell, masses of beliefs for each event of the FoD.

The constitutive classes of the FoD are also fixed at the end of the inversion process by the geophysicist, with the help of a representation of the distribution of the set of inverted geophysical values, in the form of modal classes (Figure 1.a). The representation in this form makes it possible to highlight the centers, minima and maxima of the events considered in order to be able to fix the bounds of the intervals associated with the events of the FoD. The number of cells of the subsoil section are represented according to the geophysical parameter values. The infima and suprema must be fixed so that the intervals are of the same width in order to avoid the appearance of a bias when calculating Wasserstein distances (detailed under). To associate the belief masses with the FoD events, the intervals of inverted values of the physical parameter (in red, Figure 1.b) are considered. For some geophysical methods, these intervals can correspond to the value obtained at the end of the inversion with its associated inaccuracy.

It is then necessary to associate belief mass values $m_1(.)$ corresponding to each element of 2^{Θ}, for each cell of the inverted section. The masses are obtained from the calculation of Wasserstein distances [25], considering two geophysical intervals A = [a_1, a_2] and B = [b_1 , b_2] with A and B belonging to **R**, A being the interval corresponding to an event of the FoD and B being an interval of inverted values (Figure 1.b), Eq. (10):

$$d_{Wass}(A,B) = \left[\left(\frac{a_1+a_2}{2}\right) - \left(\frac{b_1+b_2}{2}\right)\right]^2 + \frac{1}{3}\left[\left(\frac{a_2-a_1}{2}\right)^2 + \left(\frac{b_2-b_1}{2}\right)^2\right] \quad (10)$$

This calculation estimates the distance between two intervals according to their size and the distance between them. The Wasserstein distances are calculated (using a logarithmic scale if the geophysical parameter requires it) between the inverted values with estimated inaccuracies, and the intervals associated with each event, chosen by the geophysicist. Each cell is finally associated with a standardized BBA respecting Eq. (3). This way, the more the distance of a geophysical interval resulting from the inversion is "close" to one event of the FoD, the more the mass of belief associated is important, and reciprocally.

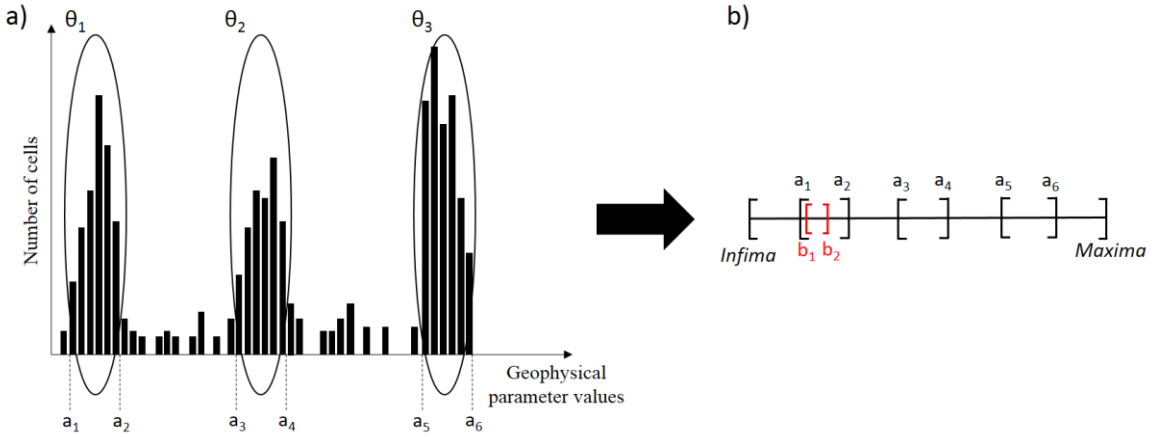

Figure 1: a) Model classes' distribution of the geophysical parameter values from the considered subsoil section, allowing the selection of the geophysical classes in b). The red interval corresponds to an interval of inverted values, from one cell of a 2D section of subsoil, used for Wasserstein distances' calculation.

Geotechnical data

For the geotechnical part, the information proposed during an investigation campaign is spatially punctual (in the x-z plane) and often contained in vertical soundings made from the surface. It is about associating masses of belief with the different events of the FoD for each cell of the considered vertical soundings. For this, the values proposed at each depth are considered with the associated inaccuracy, corresponding to the measurement error that could be attributed to the measuring device (Figure 2.a). Thus, as for the geophysical part, intervals of values are obtained.

The geotechnical mesh consisting of as many cells in depth as the number of geotechnical values (Figure 2.b) is generated. A mass of belief $m_2(.)=1$ is assigned, in the drilling points, to the events corresponding to the measured geotechnical parameter. A value of *1* is set since we are very confident in the information inside the boreholes unlike the spatialized geophysical information. A new mesh is then constructed (Figure 2.c), according to the size and depth of the boreholes. In order to characterize the entire section of the model, as does the geophysical method, and to associate mass values to each new cell (BBA), an exponential lateral decay of the belief mass is imposed, from the drilling point to the nearest borehole so that the decay rate is a function of the values proposed by the nearby borehole. So that, for a specific depth, Eq. (11):

$$BBA(x) = e^{-kC_v x}\, BBA(0) \quad (11)$$

With x being the distance from the considered cell to the reference borehole ($x=0$ in the borehole), k a decay factor fixed by the user to adjust the lateral decay rate, $BBA(x)$ the belief mass values assigned to each event of the FoD for a position x, with $BBA(0)=1$. C_v corresponds to the coefficient of variation expressed in Eq. (12), such as used in [26]:

$$C_v = \frac{\sqrt{\frac{1}{n_{mesh}-1}\sum_{i=1}^{n_{mesh}}(Q-Q_i)^2}}{Q} \quad (12)$$

Where Q is the geotechnical value of the reference cell in the considered borehole and Q_i the geotechnical value in the nearby borehole. For Figure 2.b, $n_{mesh}=3$ has been considered. If $n_{mesh} = 5$ or 7, the computation of the C_v will take into account *5* or *7* cells in the nearby borehole. Indeed, for two consecutive boreholes

with similar values, at similar depth, the decay of the confidence is slower than for two consecutive boreholes presenting radically different values. This decay of belief mass is carried out to the left and to the right, from each drilling.

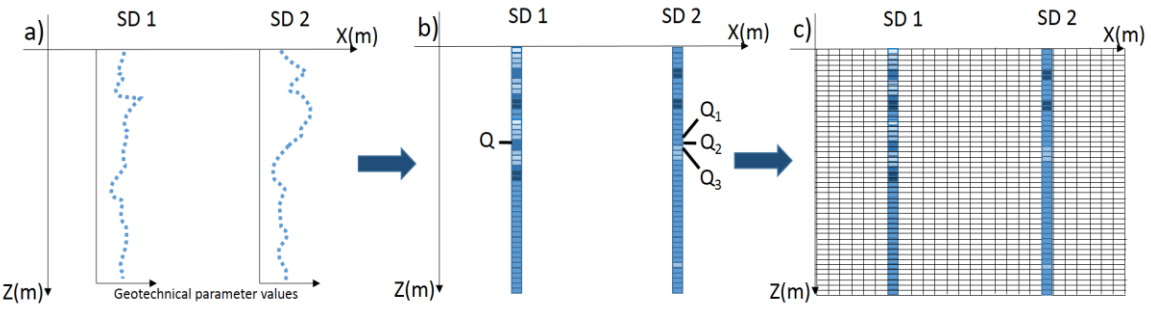

Figure 2: Construction of a geotechnical discretization mesh from two vertical boreholes acquisition (SD1 and SD2). a) Representation of the geotechnical values for SD1 and SD2 according to the depth. b) The boreholes are divided in cells associated with belief mass equal to 1 for the considered event. c) Construction of a new mesh according to the size and depth of the boreholes.

If, between two boreholes, the mass of belief associated with a hypothesis A is less than 1 *(m_2 (A) <1)*, then the remainder of mass to be allocated to satisfy Eq. (3), is reported on the proposition "any type of material" represented by the union of all events, such as Eq. (13):

$$m_2(\theta_1 \cup \theta_2 \cup \theta_3 \cup \theta_4) = 1 - m_2(A) \tag{13}$$

Considering *n* boreholes, from *1* to *n* from left to right: borehole *1* cannot be compared to any borehole to its left neither can borehole *n* be compared to any borehole to its right. Indeed, for a given depth, an equal C_v is considered for left and right directions, for boreholes located at the beginning and at the end of the section.

3) Dimensioning of the mesh prior to the fusion

Each source of information imposes its own mesh but in order to combine the belief masses from the geophysical information source (source 1) and the geotechnical source (source 2), it is necessary to have a common mesh containing, for each cell, the geophysical and geotechnical BBAs. In order to not alter the quality of the information, no interpolation is carried out. It is decided to superimpose the geophysical discretization grid resulting from the 2D inversion to the geotechnical division, depending on the number and the borehole positions. Thus, an irregular mesh is obtained but without any approximation (Figure 3).

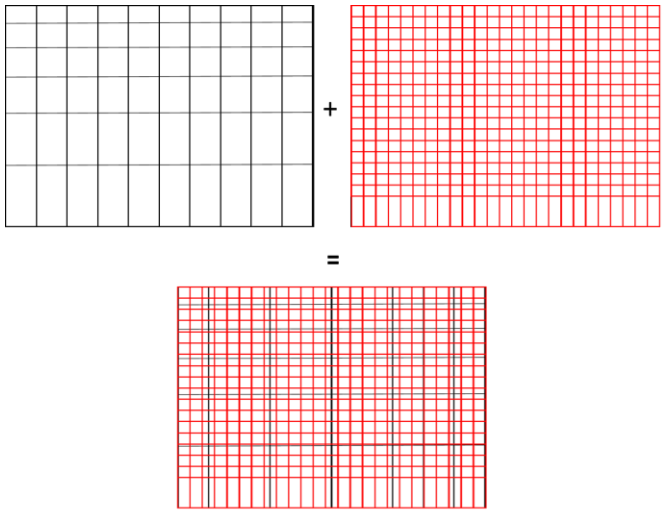

Figure 3: Example of a geophysical mesh (in black) and a geotechnical mesh (in red) superimposed to propose a new irregular mesh to carry out the combination calculations and present the fusion results.

III. Synthetic study

Below, a synthetic study based on artificial data is proposed in order to test this new proposed methodology. It is the opportunity to show the impact of different levels of noise on the geophysical information as well as the influence of the lateral decay factor k (Eq.11) on the results of the fusion in order to be able to choose a value for the use of such a methodology from real data.

1) Considered methods

For this study, the electrical resistivity tomography (ERT) method stands for the geophysical information source and the Cone Penetrometer Test (CPT) method for the geotechnical information source.

The basic principle of DC-resistivity methods consist in injecting an electric current of known intensity [A] by means of two "current" electrodes and measuring a voltage [V] between two “potential” electrodes. Depending on the electrode layout, the topography, the properties of the materials and their distribution, apparent resistivity values can be computed. The depth of investigation depends on the spacing of the electrodes, the configuration of the electrodes and the nature of the soil [27]. By generalizing this principle, a two dimensional (2D) ERT consists in aligning a series of electrodes and acquiring a large number of measurements based on four electrodes configuration. The apparent resistivity data acquired are then inverted using an inversion code or software to reconstruct a complete 2D-section of electrical resistivity [Ω.m]. Here the Res2Dinv software (ver 3.71.118) [27] has been used.

In order to obtain an artificial resistivity section of subsoil, a two steps procedure is followed. First, resistivity data are simulated using the Res2Dmod software [28], on the section that we want to consider. Second, apparent electrical resistivity values are inverted with Res2Dinv, considering a L1 norm [29] and an extended model discretization, to obtain the synthetic inverted section of electrical resistivity.

The CPT method consists in pushing rods into the soil, at a constant speed, with a conical tip at the end [30]. This test is often used for the determination of the soils mechanical resistance properties. The two measured parameters are the tip resistance q_c [MPa] and sleeve friction f_s [MPa]. Although the method uses two parameters, only q_c will be considered as the study parameter.

2) FoD and considered model

For this synthetic study, a two-layer model is considered, composed of materials that can be likened to silts for the upper layer and clays for the underlying layer. The FoD therefore contains three material class hypotheses, such as:

$$\Theta = \{\theta_1, \theta_2, \theta_3\} \tag{14}$$

With θ_1 the event corresponding to the clayey material, θ_2 to the silty material and θ_3 to unknown materials. The latter is associated with the union of the geophysical and geotechnical value ranges that do not correspond to those associated with θ_1 and θ_2. This event θ_3 allows us in a certain way, to quantify the lack of knowledge of the environment since it does not include the two first sets. The construction of the BBAs then consists in associating the data of the two considered sources to the events of the FoD. Figure 4 shows the two-layer model based on events from the FoD, used for this synthetic study.

Figure 4: Representation of the events of the FoD in the imposed model of subsoil of the synthetic study.

3) Construction of BBAs from geophysical and geotechnical data

Geophysical data

The electrical acquisition is simulated with a Wenner acquisition mode and with 96 electrodes interspaced from one meter. An electrical resistivity of 100 Ω.m is considered for the upper material and a resistivity of

30 Ω.m for the underlying one [31] (Figure 4). Electrical acquisitions are simulated with different noise levels (5, 10 and 15%). The results of this inversion (with 10% noise, figure 5.a) allow to highlight the presence of two layers but the interface between these two layers is not perfectly identified. A variation of thickness in the center of the model is visible. The interface is not straightforward and anomalies are present on the surface even though they are not part of the initial model.

From these inversion results, it is possible to define the ranges of electrical resistivities that will be associated with the different events considered for the fusion process. A distribution in modal classes is used to visualize the number of cells, in the discretized section of the 2D inversion, associated with specific range of resistivities (Figure 5.b). This distribution allows to highlight the two large material classes of the model. Thanks to it, the bounds of the considered events can thus be defined (in Ω.m), so that the intervals have the same length (in logarithmic scale):

$$\begin{gathered}\theta_1 = [25; 45] \\ \theta_2 = [83; 149.4] \\ \theta_3 = [13.89; 25[\cup]45; 83[\cup]149.4; 268.92]\end{gathered} \tag{15}$$

As explained in II.2., it is possible to associate belief masses with each cell of the mesh thanks to the values resulting from the inversion. As part of the construction of geophysical BBAs, the values presented Figure 6 are obtained. This figure highlights the association of the values of Figure 5.a with the events of the FoD, Eq. (15). The presence of a top layer (θ_2) and a base layer (θ_1) can be detected (Figure 6.a). It appears that there is a variation in the thickness of the layers in the center of the model, but the interface is not well characterized. Moreover, the intermediate values of electrical resistivity resulting from the inversion (Figure 5.a) between θ_2 and θ_1 layers induce the representation of a third material (θ_3) which has no reality in the model that has been fixed. The belief masses are maximum when the resistivity values correspond to the center of the resistivity classes set for each event (Eq.15).

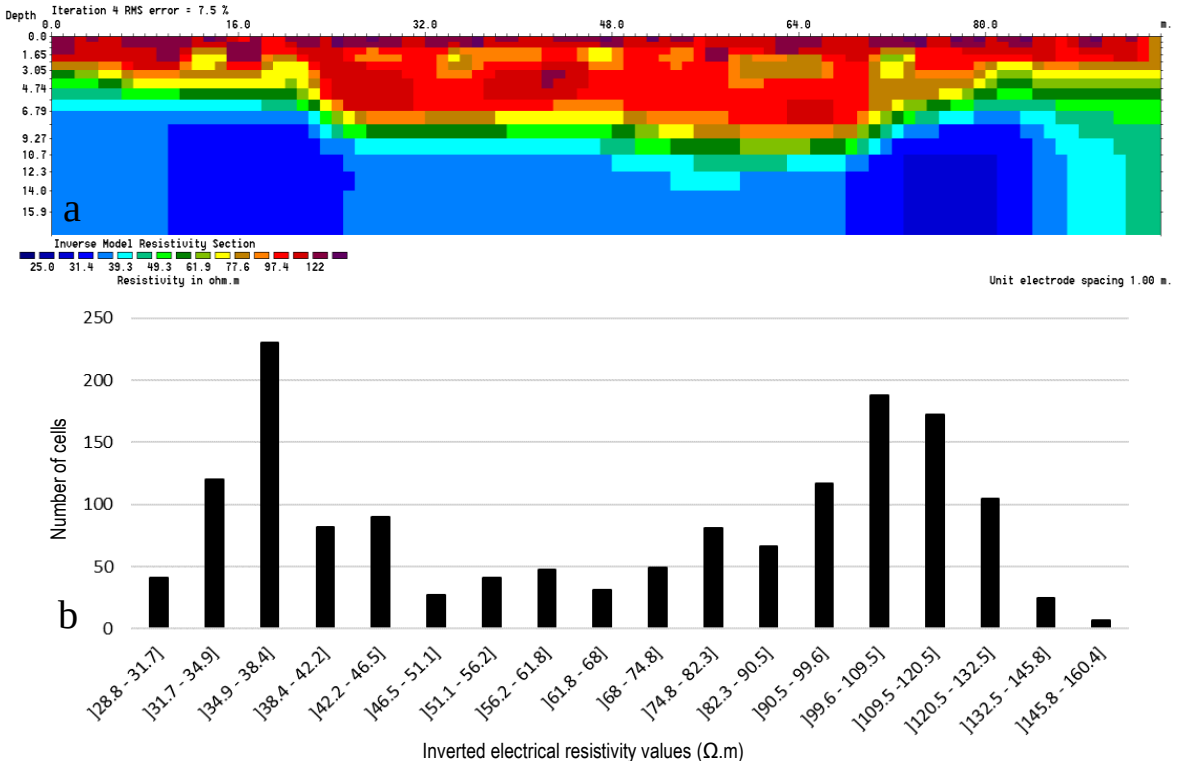

Figure 5: a) Subsoil section displaying inverted electrical resistivity values from 10% noise data acquisition and b) model classes' distribution of the cells presented in a), according to the electrical resistivity values (Ω.m).

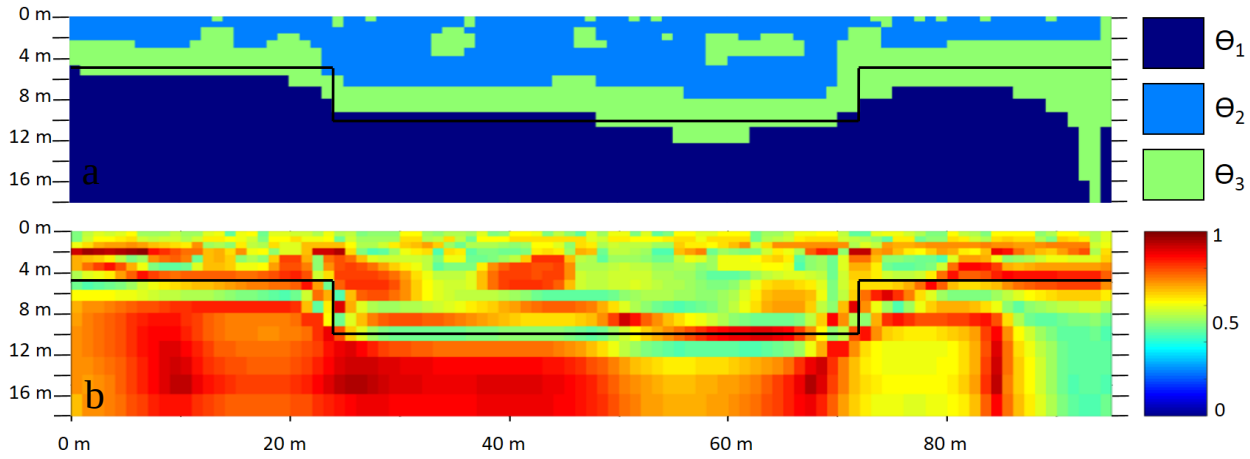

Figure 6: a) Representation of the event having the highest belief mass according to the BBA construction from geophysical data and b) the associated belief mass values, considering a 10% noise. The black line represent the position of the interface.

Geotechnical data

Concerning the source of geotechnical information, the simulation of four vertical CPT soundings inter spaced from 19 meters is proposed (Figure 7). 20 cm wide and up to 15 m deep boreholes are considered, and a value of q_c is recorded every 50 cm from the surface. An inaccuracy of 10^{-2} MPa on the measurements is considered. For a fixed normalized friction ratio of 3%, a value of q_c of 20 MPa is considered for the upper silty material and a value of 0.2 MPa for the underlying clay material, as proposed in the Robertson diagram [32].

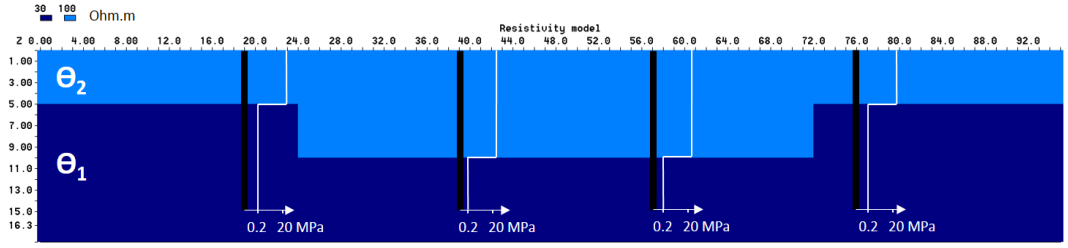

Figure 7: 2D section of subsoil displaying true ER distribution with boreholes positions in black and associated tip resistance vertical profiles in white.

In order not to have uniform values of q_c for the materials and to try to represent the noisy reality of an acquisition in the field, values are drawn following a normal distribution defined for each event. Mean q_c values of 0.2 and 20 MPa are respectively used to define the normal distributions of the material classes. Standard deviation values equal to 10% of the mean values are associated, echoing the 10% noise used for the geophysical data. Keeping the minimum and maximum values, these random draws, make it possible to define the limits, in MPa, of the intervals associated with the elements (i.e. material classes) of the FoD:

$$\begin{aligned} \theta_1 &= [0.14; 0.27] \\ \theta_2 &= [13.5; 23.5] \\ \theta_3 &= [0.1; 0.14[\cup]0.27; 13.5[\cup]23.5; 100] \end{aligned} \tag{16}$$

The minimum and maximum values are fixed at 0.1 and 100 respectively because they are the minimum and maximum values in Robertson's diagram [32].

There are two types of sounding results according to their position (Figure 8). Once the values associated with the meshes of the sounding are obtained, it is possible to associate masses of belief to the whole section by extending the geotechnical information, as explained in II.2. In the framework of the construction of geotechnical BBAs and for $k = 0.1$ (Eq.11), the obtained values are proposed in Figure 9. This figure highlights the fact that the confidence is maximum in the soundings. This method allows us to characterize the material θ_2 on the first 5 meters of the model and the material θ_1 from 10 to 15 meters deep.

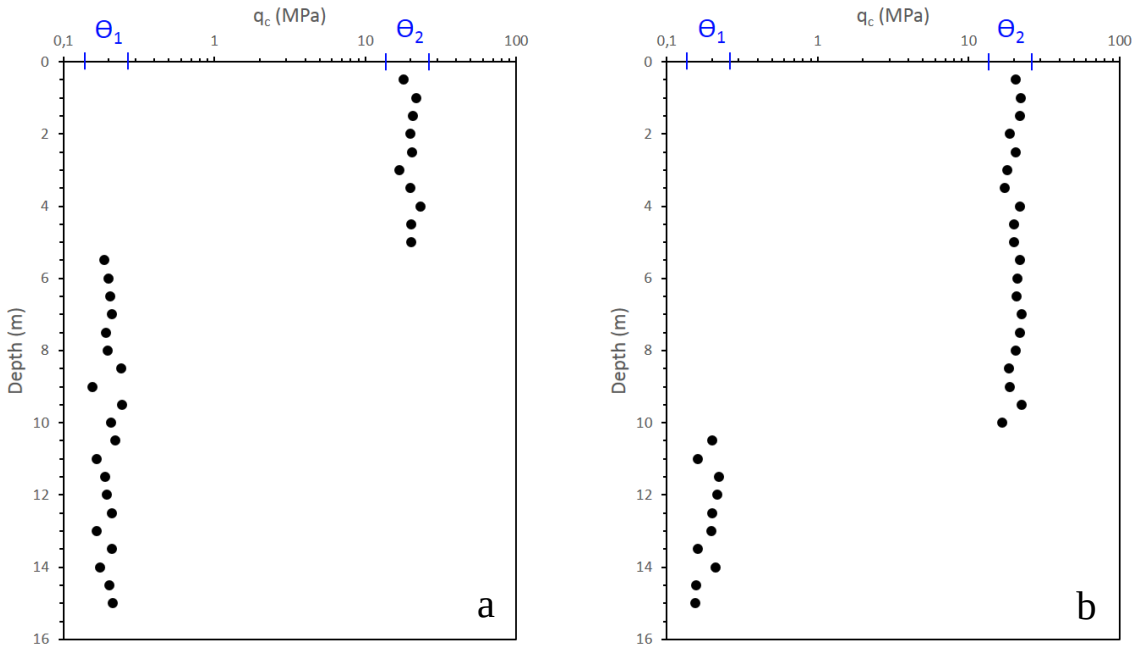

Figure 8: Examples of the two types of simulated soundings with tip resistance values according to the investigation depth. a) corresponds to borehole n°1 and 4 on figure 7 while b) corresponds to borehole n°2 and 3 on figure 7.

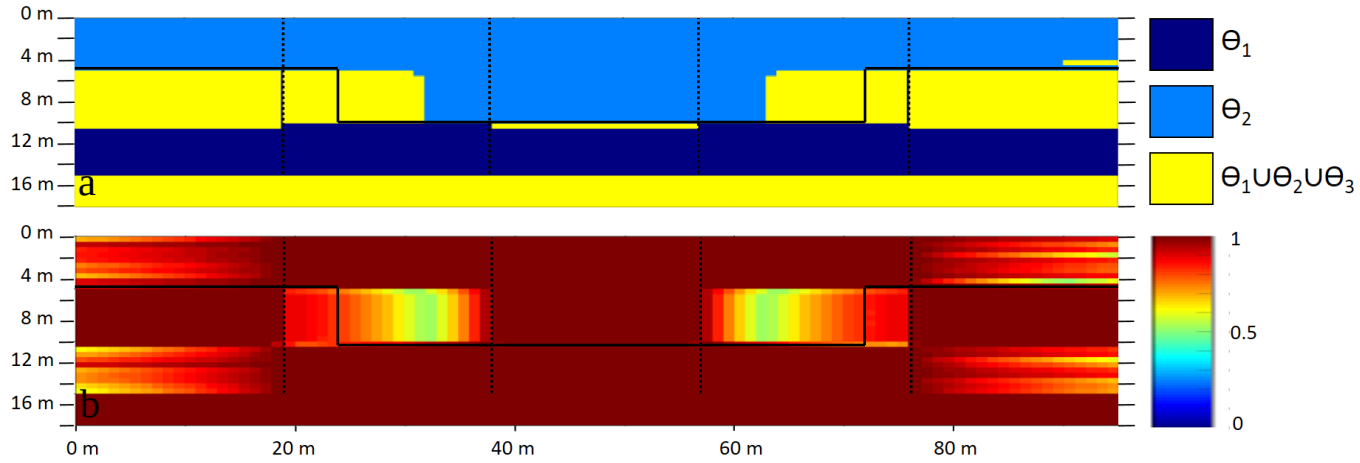

Figure 9: a) Representation of the events having the highest belief mass according to the BBA construction from geotechnical data and b) the associated belief mass values. The borehole positions are in dashed lines while the black line represent the position of the interface.

The greater thickness of the material θ_2 in the center of the model is also well characterized. On the other hand, a great doubt appears in yellow (Figure 9.a) in certain areas, not allowing the determination of a specific material ($\theta_1 \cup \theta_2 \cup \theta_3$). For the model base area, this can be explained by the fact that the soundings stop at 15 meters depth. Regarding the areas between 5 and 10 meters to the right and left of the first and last sounding, this is related to the fact that for these two soundings, the closest soundings propose different values at the same depths, the confidence attributed to the presence of θ_1 therefore decreases very quickly laterally. This decay is also high towards the edges of the model because no other sounding is present at the ends to constrain the information.

4) Effect of lateral decay factor and noise level on the fusion results

We examine in this part the results of the fusion of belief masses established for the proposed synthetic model by varying the noise level of the geophysical information, as well as the value of the lateral decay factor *k* (Eq.11) influencing the lateral decay rate of geotechnical information.

Figure 10 shows the fusion results with different values of *k* (10^{-2}, 5.10^{-2}, 10^{-1}, 5.10^{-1} and 1) for a simulated noise of 10% on the acquired geophysical information. Noise was set at 10% since the electrical resistivity classes of the FoD were defined from the modal classes of the inverted 10% noise image, Figure 5.b. For each value of *k*, Figures 10.a and 10.b represent the results obtained by Smets fusion whereas Figures 10.c and 10.d represent the results obtained by PCR6 fusion. While Figures 10.a and 10.c show the material classes having the greatest mass of belief at the end of the fusion process, Figures 10.b and 10.d correspond to the values of these respective belief masses, between 0 and 1. These figures, display the events (materials) potentially present within the section, as well as their attached level of confidence.

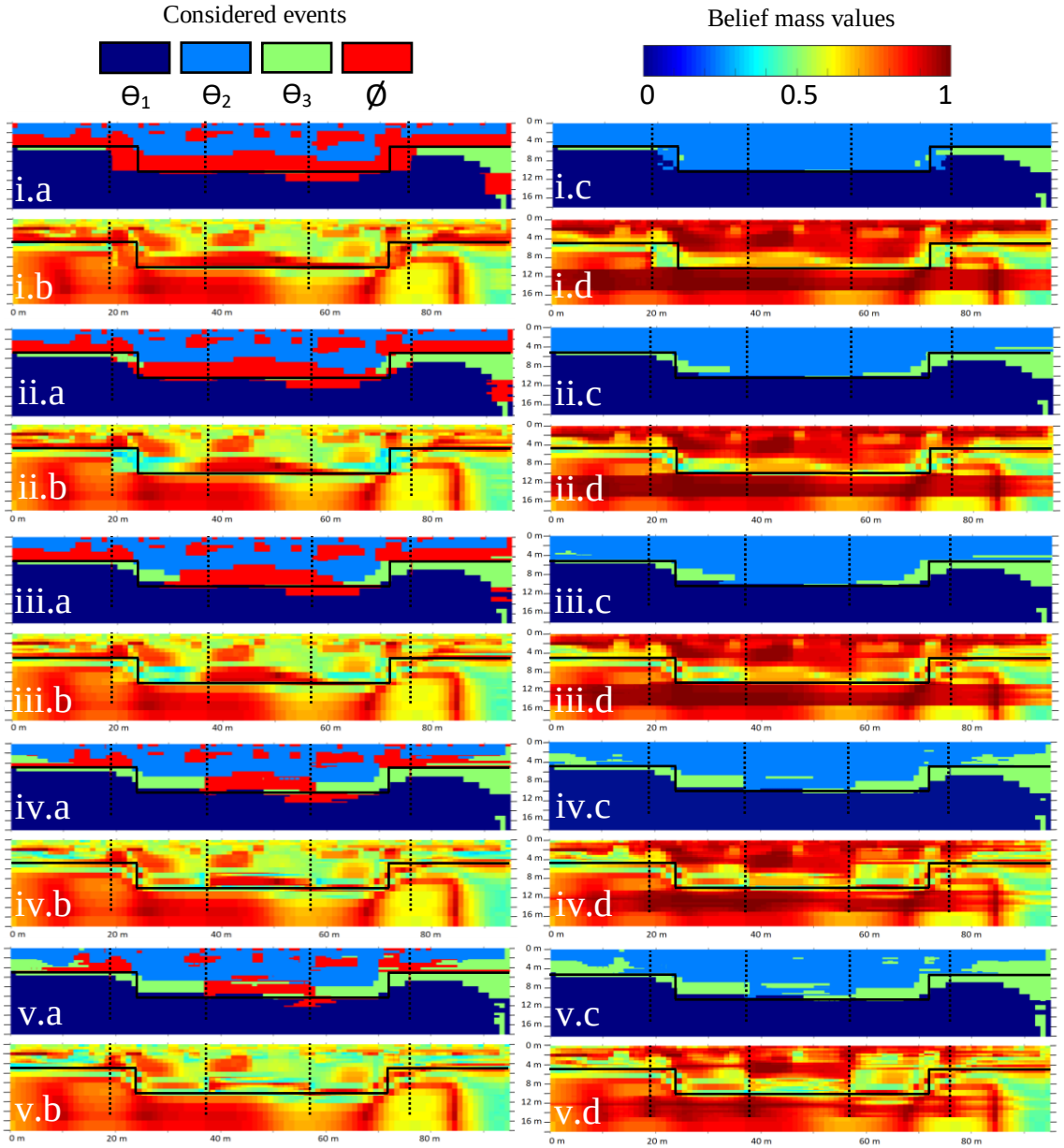

Figure 10: Representation of the events having the highest belief mass in a) and c) and their associated mass values in b) and d), considering a 10% noise. In i) k=0.01, ii) k=0.05, iii) k=0.1, iv) k=0.5 and v) k=1. Figures on the left side are results for Smets fusion while figures on the right side are results for PCR6 fusion. The sounding positions are in dashed lines while the black line represent the position of the interface.

The higher the value of *k* is, the higher the rate of confidence in geotechnical information is. This can be seen, for example, from the last borehole to the right end of the section (Figures 10.b) or between the 2nd and

3rd boreholes (Fig 10.d). The increase of *k* implies that for two soundings offering similar values at the same depth, the confidence associated with the corresponding type of material will tend to decrease. On the other hand, for two soundings proposing different values at the same depth, the increase of *k* will hardly have any impact on the belief masses associated with the selected events (e.g. between 5 and 10 m of depth between the boreholes 1 and 2, Figures 10.d).

With regard to the material classes identified after the fusion process, the more *k* increases, the more the quantity of conflict decreases (in red, Figures 10.a). This is explained by the fact that when there is little trust in the geotechnical data, there is little conflict with the geophysical data. In the meantime, an increase in the proportion of θ_3 is observed (Figures 10.c) close to the interface. This observation is explained by a larger mass attributed to the union of events and by geophysical data which propose intermediate values at the interface level.

In the following of this work, an intermediate value of *k* will be retained, equal to 0.1. With such parameter value, a good confidence in information repeating between two successive soundings is obtained, but it also leaves room for doubt by having enough unknown material (θ_3) at the interfaces. The obtained fusion results with different noise levels added to the geophysical information (5, 10 and 15%) are shown in Figures 10.iii and 11 with *k = 0.1*.

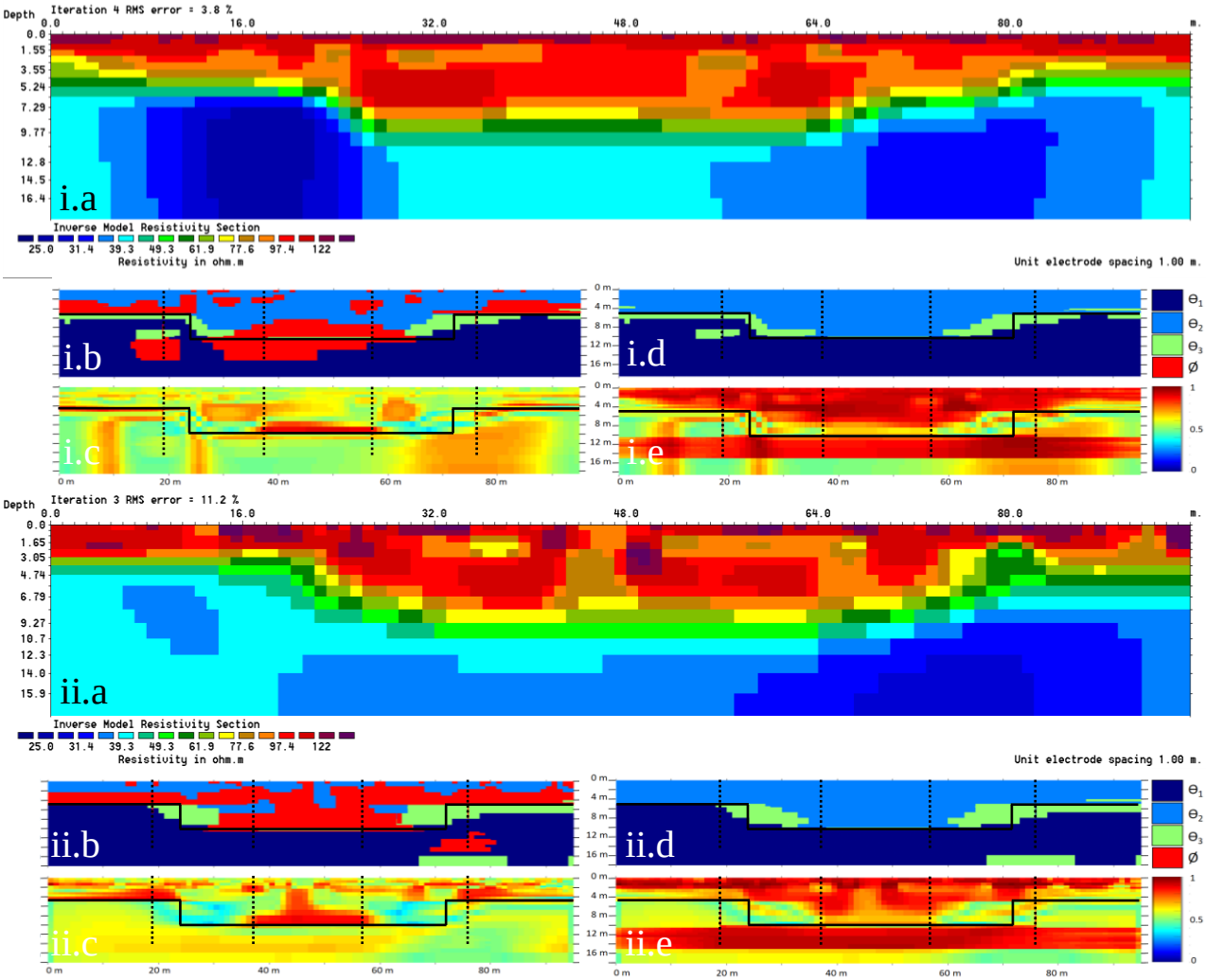

Figure 11: a) Subsoil section displaying inverted electrical resistivity values from i) 5% noise and ii) 15% noise data acquisition. Representation of the events having the highest belief mass in b) and d) and their associated mass values in c) and e). Figures on the left side are results for Smets fusion while figures on the right side are results for PCR6 fusion. The sounding positions are in dashed lines while the black line represent the position of the interface.

The greater the amount of noise is, the less clear the interfaces proposed by the inversion are (Figures 5.a, 11.i.a, 11.ii.a). A greater number of anomalies are also present when the noise level increases. The noise level finally impacts the level of inaccuracy associated with the geophysical data used in the fusion process. Larger data inaccuracies induce wider value ranges considered for calculating Wasserstein distances, which in turn can bring to consider belief masses on more events of the FoD.

Since the classes associated with FoD elements were fixed from the values with 10% noise (section III.3 and Figure 4.b), it is "reasonable" to have a higher confidence (higher belief masses) on these results than on the results with 5% and 15% noise (Figures 11.c, 11.e, 10.iii.b, 10.iii.d). The fusion process allows to override the noise effects, whether the noise level is 5 or 15%. This can be imputed to the computation of Wasserstein distances, taking into account the data inaccuracies and considering all geophysical classes.

IV. Setting up a test bench for real geotechnical and geophysical acquisitions

A. Materials

In order to be able to assess the validity of the developed fusion methodology, two methods of data acquisition were retained: (i) a mini-ERT device acting as the geophysical source of information and (ii) a laboratory penetration cone acting as the geotechnical source of information. Before setting up the test bench, it was necessary to select the materials that could be put in place in a tank in order to carry out the study. This selection implies that the materials used meet several conditions in order to validate the methodology: they must have (i) distinct electrical resistivity ranges, (ii) distinct penetration depths and (iii) a certain homogeneity in the space to limit uncontrolled anomalous values.

1) Mini ERT device

Expressly for the purposes of this study, a mini ERT device (Figure 12) has been set up. This device consists of 48 electrodes of 6 mm length, positioned at regular intervals of one centimeter. It can be moved along the test bench to make multiple acquisitions and to cover a longer section.

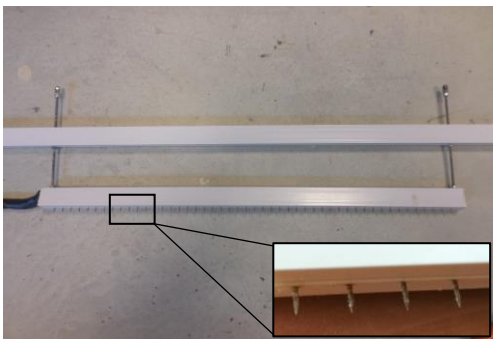

Figure 12: Mini ERT device with 48 electrodes spaced 1 cm, adjustable height, used for electrical acquisitions in the test bench.

2) Laboratory penetration cone

The laboratory penetration cone method is described in the French standard NF P 94-052-1 [33]. It consists in measuring a penetration depth of a cone, in millimeters, subjected to its own weight (Figure 13). The materials are tested individually, repeatedly, to determine an average value and a standard deviation of penetration depth for each material. These values can be used later in the study to simulate different drilling positions within the test bench. This method can be likened to the CPT method which is one of the most popular in situ geotechnical tests.

Figure 13: Laboratory penetration cone

3) Test bench and used materials

For the validation of the methodology, we wanted to build a test bench that could be easily set up and controlled, with two or three layers and variation of the interface positions. Fast-hardening natural fine-grained plaster as well as Hostun fine sand [34] are the retained constituents. These two materials meet the three conditions listed above. They were placed in a transparent PVC tank of 100 × 30 × 17 cm^3 as shown in Figure 14 with an underlying layer of 5 cm of plaster (setting time = 69 h) overlaid by a layer of 2.5 cm of water saturated sand.

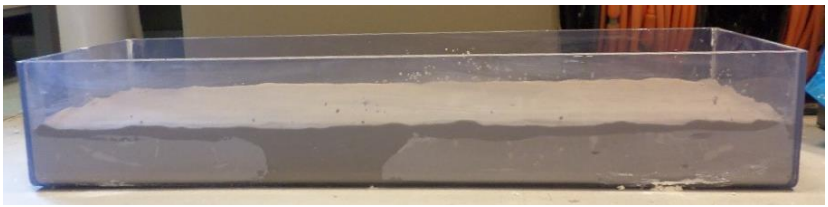

Figure 14: Transparency view of the test bench

A formwork was made during the placement of the plaster so that a 20 cm long anomaly could be inserted in. Saturated sand of 7.5 cm thickness is present instead of plaster. The contact between the materials and the bottom of the tank is at the origin of an interface that will be interesting to detect with the help of the methodology. 16 kg of plaster were mixed with 8 kg of water to obtain the material finally put in place. The electrical resistivity of the plaster was measured before and after the placement of the saturated sand to verify that the presence of water had a negligible impact on the electrical properties of the plaster.

Table 1: Values of electrical resistivity and depth of penetration of the materials set up within the test bench

	Plaster before pluviation	Saturated Hostun sands
Electrical resistivity (Ω.m)		
Mean	31.28	78.15
Standard deviation	3.23	11.18
Number of measures	12	52
Penetration depth (mm)		
Mean	0.11	17.31
Standard deviation	0.04	1.61
Number of measurements	8	10

For the Hostun sand, 15.82 kg were pluviated in 5.8 kg of water, above the plaster to reach saturation. Trials had been carried out in advance to determine the proportions of water and sand required to achieve such a state as well as to validate the repeatability of such installation by pluviation. The values of electrical resistivities and penetration depths are displayed in Table 1.

B. FoD and BBA modeling

1) FoD and target model

A FoD consisting of four elements (material classes) is considered so that:

$$\Theta = \{\theta_1, \theta_2, \theta_3, \theta_4\} \tag{17}$$

With θ_1 the element corresponding to the plaster material; θ_2 corresponding to saturated sand; θ_3 corresponding to the hard and electrically insulating bottom of tank simulating a substrate and θ_4 corresponding to unknown materials, being the union of the ranges of values not corresponding to those associated with the 3 previously described materials. Figure 15 presents the target model in the form of events constituting the FoD, following the disposition of the materials within the test bench. Although the tank used is 1 m long, the ERT acquisition only covered a 83 cm long section, on the central line of the model, and allowed us to image up to 18 cm of depth.

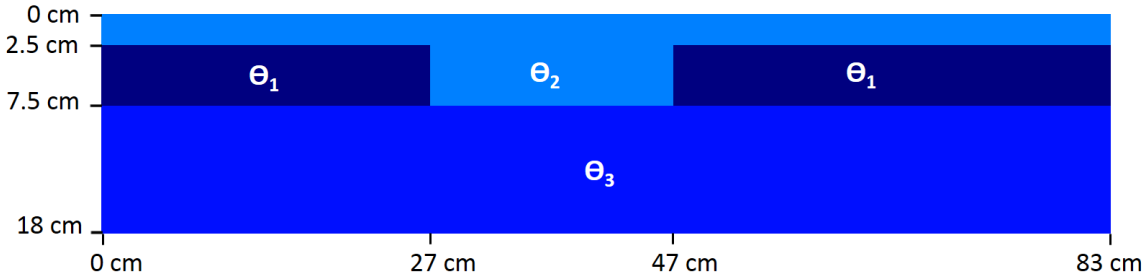

Figure 15: Scheme of the idealized section model (with vertical exaggeration), including the FoD constituent events associated with the materials of the test bench

2) Construction of BBAs from geophysical and geotechnical data

The electrical acquisition was carried out on 83 cm long, on the central line of the model, with a first acquisition on 47 cm, and three next acquisitions done after respective displacements of 12 cm (roll along method). The results obtained from the inversion of the acquired data are displayed in Figure 16.a. These results make it possible to highlight the existence of three distinct sets, at depths relatively close to the target model (Figure 15) but presenting vertically slightly shifted interfaces, gradual rather than sharp. In addition, the variation in saturated sand thickness is poorly evaluated. Indeed, the anomalous zone is recognized but associated here, in its lower part, with values of electrical resistivities much larger than what they really are.

The proposed values, although in the same order of magnitude, do not exactly match the ranges of values measured on the materials independently (Table 1). In order to characterize the events (materials) of the FoD, a distribution in modal classes (Figure 16.b) is used to visualize the number of cells of the discretized section for the 2D inversion, associated with their corresponding ranges of resistivities. This distribution makes it possible to highlight the three large sets of materials in the model. Thanks to it, the bounds of the events considered can thus be defined, in Ω.m, so that the intervals are the same length, as presented Eq. (18):

$$\begin{gathered} \theta_1 = [10; 35] \\ \theta_2 = [40; 140] \\ \theta_3 = [9\,500; 33\,250] \\ \theta_4 = [2.85; 10[\cup]35; 40[\cup]140; 9\,500[\cup]33\,250; 116\,375] \end{gathered} \tag{18}$$

In contrast to information from the geophysical source, geotechnical data were obtained beforehand by laboratory penetration cone testing, and then numerically simulated prior to fusion. Several simulations proposing various positions of survey points were carried out. In order to simulate drilling points, the associated mean depth values (mm) and associated standard deviations (Table 1) were used to draw values,

following a normal distribution defined for each event. An average penetration depth value of 0 mm is used for θ_3 (bottom of tank) and an associated standard deviation of 0.01 mm, meaning that negative values may be drawn. These random draws, make it possible to define the limits, in mm, of the intervals associated with the events of the FoD as presented Eq. (19):

$$\begin{gathered}\theta_1 = [0.04; 0.19] \\ \theta_2 = [13; 21] \\ \theta_3 = [-0.02; 0.02] \\ \theta_4 = [-0.05; -0.02[\cup]0.02; 0.04[\cup]0.19; 13[\cup]21; 100]\end{gathered} \tag{19}$$

Thus, 2 mm wide boreholes are simulated, down to 15 cm and acquiring every 5 mm with an associated inaccuracy of 0.01 mm. The values of penetration depth obtained can then be associated with the different materials of the model.

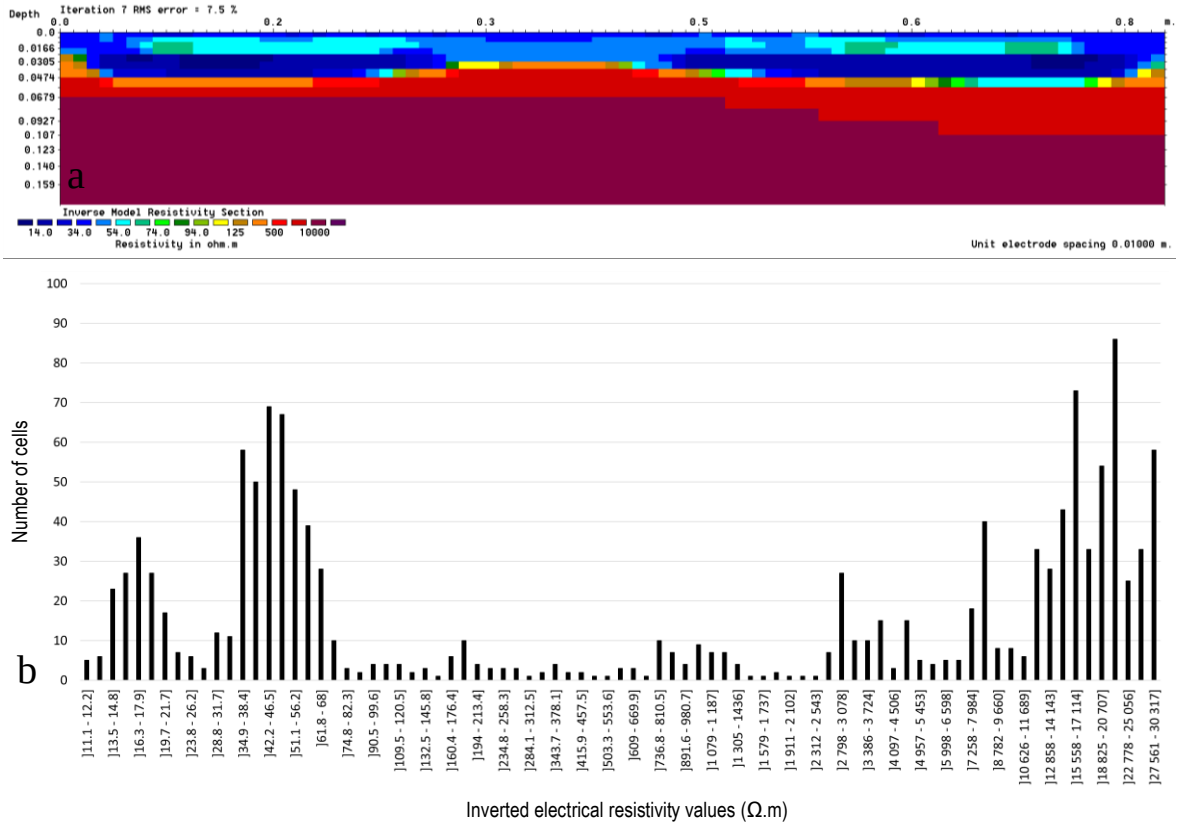

Figure 16: a) inverse model resistivity section obtained by roll along acquisitions in the central line of the model and b) model classes' distribution of the cells presented in a), according to the electrical resistivity values (Ω.m).

V. Test bench data fusion results

The results of the geophysical and geotechnical information fusion, are proposed in Figure 17. The simulations were carried out according to four distinct vertical drill positioning configurations, represented in dashed lines in the figures and at regular intervals: i) 8 holes inter-spaced of 10 cm (Figure 17.i) (x = 10; 20; 30; 40; 50; 60; 70; 80 cm), ii) 5 holes inter-spaced of 18 cm (Figure 17.ii) (x = 4, 22, 40, 58, 76 cm), iii) 3 holes inter-spaced of 25 cm (Figure 17.iii) (x = 15, 40, 65 cm)), iv) 2 holes inter-spaced of 50 cm (Figure 17.iv) (x = 15, 65 cm). The fusion results carried out are presented, respecting i) the hypothesis of Smets (Figures 17.a and 17.b), ii) the hypothesis of a closed-world (section II.1) with PCR6 rule (Figures 17.c and 17.d). Figures 17.b and 17.d represent the belief mass values associated with events having the largest mass, represented respectively in Figures 17.a and 17.c. The fusion results are analyzed and discussed in the next section.

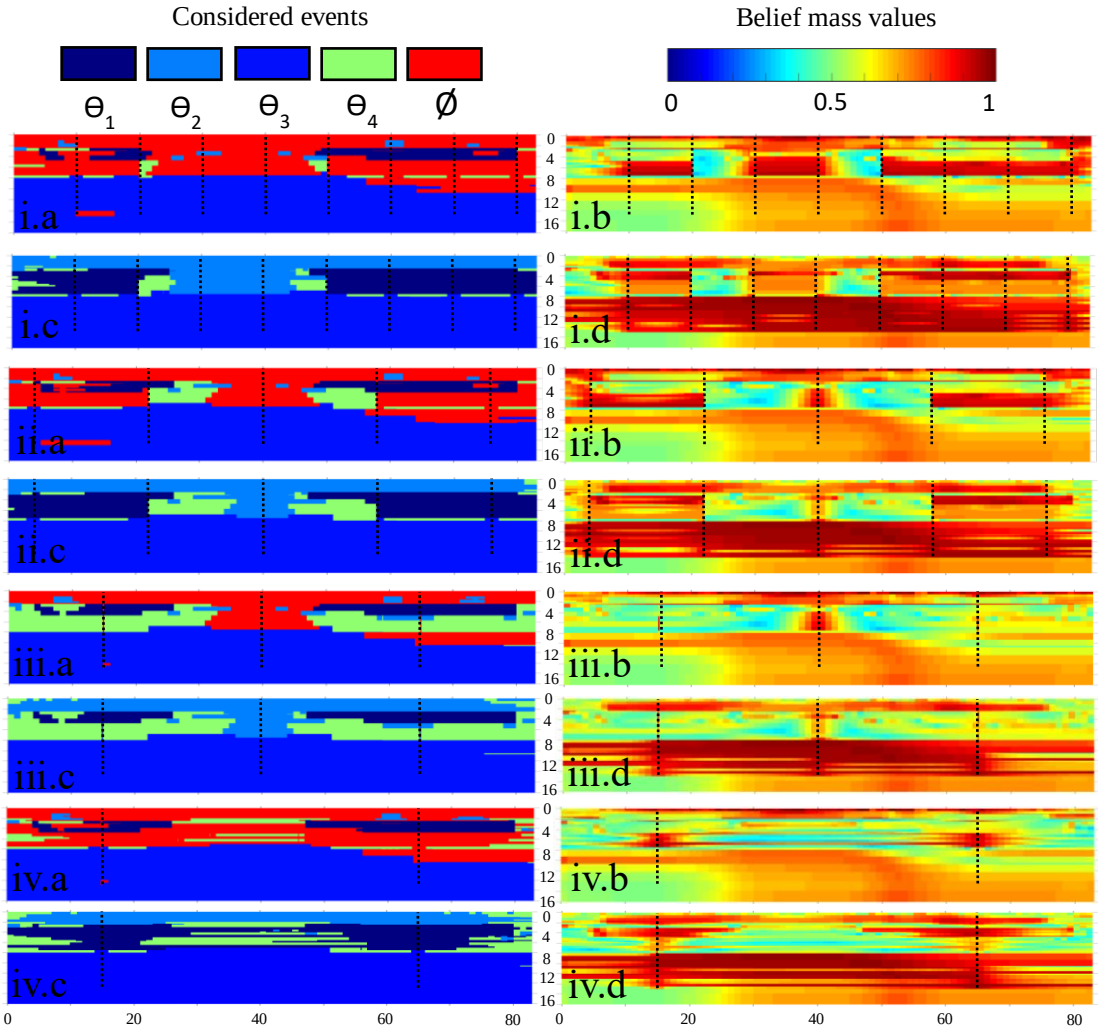

Figure 17: Representation of the events having the highest belief mass in a) and c) and their associated mass values in b) and d). For i) 8 boreholes, ii) 5 boreholes, iii) 3 boreholes, iv) 2 boreholes are considered. For each case, (a,b) figures are results of Smets fusion, while (c,d) figures are results of PCR6 fusion. The borehole positions are in dashed lines.

VI. Fusion results analysis and discussion

Different rules of combinations

Let us discuss and compare the results obtained by the 2 different combination rules used in an 8-boreholes simulation (Figure 17.i). In the framework of a model as rich in geotechnical information, the section proposed by the PCR6 method (Figure 17.i.c) is very close to the target model set up (Figure 15). The three sets are well characterized and the interfaces at 2.5 cm deep (sands-plaster) and at 7.5 cm deep (plaster-PVC tank and sand-PVC tank) are much better defined than by ERT alone (Figure 16.a). Moreover, thanks to this geotechnical information, the sand thickness anomaly could be correctly characterized as saturated sands (θ_2) and not as a more resistive anomaly, in continuity with the insulating material from below, as suggested by the results of the inversion. The lateral extension of this anomaly is, moreover, well estimated (20 cm). The combination of Smets highlights the significant conflict existing between the two considered sources of information (Figure 17.i.a) concerning the two first layers.

Whatever method is used, the presence of a hypothesis θ_4 is found at the vertical and horizontal interfaces (Figures 17.i.a, i.c). This hypothesis does not correspond to any material set up in the test bench. The belief masses attributed to such a hypothesis, highlight the transition zones not conform to reality, proposed by the inversion of the electrical resistivity data (Figure 16.a). In comparison to the belief masses associated with the other hypotheses of the model, the belief masses associated with θ_4 are the lowest (Figures 17.i.b, i.d),

showing that the confidence granted to such a material remains quite relative. An overall confidence drop is also observed from 15 cm depth. This corresponds to the maximum depth reached by the simulated boreholes. As confidence is extended laterally, the belief masses are constrained only by geophysical information to such a depth and therefore rely only on one source of information.

Influence of the number of boreholes and positions

The first intuition would be to assume that the more the number of boreholes decreases, the more the method should be put in difficulty to properly characterize the section of the set up test bench. Although this is partly true, the quality of the results is not based as much on the number as on the positions of the drillings. Indeed, the anomaly of saturated sands contained between the two banks of plaster (Figure 15) is as well characterized in terms of lateral extension with three or five soundings (Figures 17.ii.c, iii.c). It also has an equivalent associated trust (Figures 17.ii.d, iii.d). It turns out that the belief masses associated with the event θ_1 (plaster) are even smaller for a fusion including three soundings (Figures 17.iii.d) than for a simulation of only two (Figures 17.iv.d).

The explanation of such results lies in the fact that being in the presence of consecutive boreholes, informing about the occurrence of different materials, at an equivalent depth, induces a rapid decrease in the confidence attributed to the boreholes. Therefore, more credibility is given to the geophysical information source, explaining the greater presence of θ_4, which reflects the gradual transitions in electrical resistivities. The masses associated with this event, however, remain relatively small. On the other hand, if two consecutive boreholes have the same geotechnical values, for a specific depth, the lateral decay rate will be low and no priority can be given to a different material existing between these two boreholes. That is why the sand anomaly in the center of the model does not appear in the results fusion with two soundings (Figures 17.iv.c) : no borehole pass through the anomaly and the geophysical source is unable to characterize this material as saturated sand. The strength of these results is that they suggest the presence of θ_4 in this location, suggesting that the survey campaign should be reinforced (with a new borehole position for example).

The conflict presented by Smets combination (results in Figures 17.i.a, ii.a, iii.a and iv.a) is neither a function of the number of geotechnical soundings. In this study, the cases of fusion bringing the highest amount of conflict are in fact the ones with eight and two soundings. Nor is it to be confused with a lack of knowledge of the subsoil. Conflict zones highlight contradictory information between the two sources. These zones are generally between two consecutive boreholes providing the same information, but going against the available geophysical information. These are therefore potentially anomalous zones where the geophysical information must be considered carefully, in particular if the belief mass associated with the event retained after normalization is too low.

Important considerations and potential in the application

It is important to consider that the effectiveness of this fusion methodology has been assessed by comparing the fusion results with a target model (Figure 15). However, this remains an idealized representation of the test bench set up and could be, in some places, quite far from reality (real interfaces not perfectly horizontal or vertical, materials not perfectly homogeneous, 3D effects neglected ...). The approach is different from the one of the synthetic study (Figure 4) where the model shown corresponds to the true model. In order to control the effectiveness of the fusion methodology, it was envisaged to carry out ex post verifications of the constituent materials. Unfortunately, for practical reasons, this could not be done (reworking of materials modifying their physical properties, interaction with water, delicate cutting and extraction ...).

Regarding the fusion methodology developed, two aspects are debatable. First, the choice to set a mass of belief equal to 1 on the geotechnical information in the boreholes. Second, the effect of different random draw results on the fusion results. The choice of a maximum punctual confidence (m=1) in boreholes is defended in order to give a full and local confidence to geotechnical information as it is currently done during investigation campaigns. Excessive risks are not taken since the test bench is relatively well known and the synthetic model is perfectly well known. Thus, it is sure that simulated borehole values refer to the right materials. Furthermore, a value of m=0.99 instead of m=1, for instance, does not significantly change the results and does not change the interpretation and the resulting discussion. Regarding the effect of random draws, these draws were done following a normal distribution, the variations from one draw to another are minimal and the results of fusion differ little.

Such an information fusion algorithm, dedicated to the combination of data from geophysical and geotechnical sources, should prove useful for processing of data acquired during investigation campaigns for many different kinds of issues. It is possible to envisage its use with a larger number of materials, but also,

and especially, with a larger number of data types from geophysical methods (seismics, ground penetrating radar) and geotechnical testing methods (penetration cone, core sampling with laboratory identification, permeability tests ...) associated.

In the framework of a recognition campaign, the conflict zones, or zones with a low associated confidence, would make it possible to specify the locations where the investigation must be reinforced. The ultimate goal is to obtain a more robust and cost-effective diagnosis of the investigated structure, more targeted for geotechnical investigation. This methodology has particularly shown its ability to correctly characterize interfaces, which corresponds to areas where the risk of instability is potentially the greatest. For a levee embankment issue, for example, the results from such a methodology could come to feed into models of breakage risks (ex: CARDigues [35]).

VII. Conclusion

In this work, a new methodology has been presented, based on belief functions to take benefit and to combine two different and complementary kinds of information: geophysical and geotechnical. Each one having its own spatial distribution and related uncertainties and inaccuracies. A new representation of the information has been proposed, taking into consideration two different investigation methods, associated with degrees of belief. This representation is more informative than data superposition of different physical parameters.

In the first place, this new approach has been validated with a synthetic study, simulating data acquired by ERT and a CPT method, considering a 2D model with two layers and thickness variation. The results were obtained with different noise ratios applied to the geophysical data and different values of lateral decay coefficient for the geotechnical information. The most appropriate value to pick up for the coefficient has been pointed out and it has been showed that this approach was able to manage the noise ratio, thanks to the use of Wasserstein distances.

In order to address the problem of combining information acquired by geophysical and geotechnical methods during investigation campaigns, and to acquire values from real devices, a test bench composed of plaster and saturated sands was set up. The methods used to characterize such a physical model were the ERT method (geophysical) and the laboratory penetration cone method (geotechnical). While the data has been acquired by a dedicated small scale ERT device, on the surface and on the central line of the complete model, borehole were simulated respecting the penetration depth ranges previously established.

Fusion results were proposed following 2 combination rules (Smets and PCR6) as well as for four different simulations of number and positions of boreholes. The results highlighted the ability of this fusion approach to correctly characterize the test bench materials as well as to specify the positions of the interfaces (vertical and horizontal) between the materials. Moreover, for each result, thanks to a graphical representation, the associated confidence is proposed.

Further research should include cases of material mixtures and cases of different materials sharing common ranges of physical properties in order to test the ability of this methodology to differentiate them. We also wish to test this new methodology in real investigation campaigns in order to improve the available knowledge and strengthen the characterization. The level of confidence associated with the proposed results may be very relevant for decision support (eg models of failure hazards). The results of such a methodology should make it possible to propose the most relevant borehole positions (that are a function of conflictual and anomalous areas), in order to make the quality of the information more cost-effective.

Acknowledgments

We would like to thank Quiterie Forquenot de la Fortelle and Gautier Gugole for their precious help throughout the experimental phase and also would like to thank the *Région Pays de la Loire* for their financial support.

References

[1] Caris, J. P. T., & Van Asch, T. W. (1991). Geophysical, geotechnical and hydrological investigations of a small landslide in the French Alps. *Engineering Geology, 31(3-4), 249-276.*

[2] Merritt, A. J., Chambers, J. E., Murphy, W., Wilkinson, P. B., West, L. J., Gunn, D. A., Meldrum, P.I.,

Kirkham, M. & Dixon, N. (2014). 3D ground model development for an active landslide in Lias mudrocks using geophysical, remote sensing and geotechnical methods. *Landslides, 11(4), 537-550.*

[3] Chambers, J., Meldrum, P., Gunn, D., Wilkinson, P., Merritt, A., Murphy, W., West, J., Kuras, O., Haslam, E., Hobbs, P., Pennington, C., & Munro, C. (2013). Geophysical-geotechnical sensor networks for landslide monitoring. *Landslide Science and Practice, 289-294.* Springer, Berlin, Heidelberg.

[4] Abidin, Z., Hazreek, M., Saad, R., Fauziah, A., Wijeyesekera, C., Baharuddin, T., & Faizal, M. (2012). Integral analysis of geoelectrical (resistivity) and geotechnical (SPT) data in slope stability assessment. *Academic Journal of Science, 1(2), 305-316.*

[5] James, N., Sitharam, T. G., Padmanabhan, G., & Pillai, C. S. (2014). Seismic microzonation of a nuclear power plant site with detailed geotechnical, geophysical and site effect studies. *Natural hazards, 71(1), 419-462.*

[6] Coker, J. O. (2015). Integration of Geophysical and Geotechnical Methods to Site Characterization for Construction Work at the School of Management Area, Lagos State Polytechnic, Ikorodu, Lagos, Nigeria. *International Journal of Energy Science and Engineering, 1(2), 40-48.*

[7] Perri, M. T., Boaga, J., Bersan, S., Cassiani, G., Cola, S., Deiana, R., Simonini, P., & Patti, S. (2014). River embankment characterization: The joint use of geophysical and geotechnical techniques. *Journal of Applied Geophysics, 110, 5-22.*

[8] Royet P., Palma Lopes S., Fauchard C., Mériaux P., & Auriau L. (2013). Rapid and cost-effective dike condition assessment methods: geophysics. *Geography, 32(4), 1-17.*

[9] Shaaban, F., Ismail, A., Massoud, U., Mesbah, H., Lethy, A., & Abbas, A. M. (2013). Geotechnical assessment of ground conditions around a tilted building in Cairo–Egypt using geophysical approaches. *Journal of the Association of Arab Universities for Basic and Applied Sciences, 13(1), 63-72.*

[10] Foster, M., Fell, R., & Spannagle, M. (2000). The statistics of embankment dam failures and accidents. *Canadian Geotechnical Journal, 37(5), 1000-1024.*

[11] Shafer G. (1976). A Mathematical Theory of Evidence. *Princeton University Press.*

[12] Dempster A. P. (1967). Upper and lower probabilities induced by a multivalued mapping. *The annals of mathematical statistics, 325-339.*

[13] Binaghi, E., Luzi, L., Madella, P., Pergalani, F., & Rampini, A. (1998). Slope instability zonation: a comparison between certainty factor and fuzzy Dempster–Shafer approaches. *Natural hazards, 17(1), 77-97.*

[14] Althuwaynee, O. F., Pradhan, B., & Lee, S. (2012). Application of an evidential belief function model in landslide susceptibility mapping. *Computers & Geosciences, 44, 120-135.*

[15] Tangestani, M. H., & Moore, F. (2002). The use of Dempster–Shafer model and GIS in integration of geoscientific data for porphyry copper potential mapping, north of Shahr-e-Babak, Iran. *International Journal of Applied Earth Observation and Geoinformation, 4(1), 65-74.*

[16] Mogaji, K. A., Lim, H. S., & Abdullah, K. (2015). Regional prediction of groundwater potential mapping in a multifaceted geology terrain using GIS-based Dempster–Shafer model. *Arabian Journal of Geosciences, 8(5), 3235-3258.*

[17] Tehrany, M. S., & Kumar, L. (2018). The application of a Dempster–Shafer-based evidential belief function in flood susceptibility mapping and comparison with frequency ratio and logistic regression methods. *Environmental Earth Sciences, 77(13),490.*

[18] Martin, A., Osswald, C., Dezert, J., & Smarandache, F. (2008). General combination rules for qualitative and quantitative beliefs. *Infinite Study.*

[19] Cooke, R. (1991). Experts in uncertainty : opinion and subjective probability in science. *Oxford University Press on Demand.*

[20] Smets P. (1990). The combination of evidence in the transferable belief model. *IEEE Transactions on pattern analysis and machine intelligence, 12(5), 447-458.*

[21] Dezert J., Wang P., & Tchamova A. (2012), On The Validity of Dempster-Shafer Theory. *Information Fusion (FUSION), 15th International Conference on. IEEE, 655-660.*

[22] Smarandache F., & Dezert J. (2009). Advances and applications of DSmT for information fusion. 30 *Collected works - ARP Volume 3.*

[23] Smarandache, F., & Dezert, J. (2005, July). Information fusion based on new proportional conflict redistribution rules. In *2005 7th International Conference on Information Fusion* (Vol. 2, pp. 8-pp). IEEE.

[24] Kearey P., Brooks M., & Hill I. (2013). An introduction to geophysical exploration. *John Wiley & Sons.*

[25] Tran, L., & Duckstein, L. (2002). Comparison of fuzzy numbers using a fuzzy distance measure. *Fuzzy sets and Systems, 130(3), 331-341.*

[26] Phoon, K. K., & Kulhawy, F. H. (1999). Characterization of geotechnical variability. *Canadian Geotechnical Journal, 36(4), 612-624.*

[27] Loke M. H. (2011). Tutorial 2-D and 3-D electrical imaging surveys. *Technical report.*

[28] Loke, M. H. (2002). RES2DMOD ver. 3.01: Rapid 2D resistivity forward modelling using the finite difference and finite-element methods. *Software manual*.

[29] Loke, M. H., Acworth, I., & Dahlin, T. (2003). A comparison of smooth and blocky inversion methods in 2D electrical imaging surveys. *Exploration Geophysics, 34(3), 182-187*.

[30] ISO 22476-1:2012(en) Geotechnical investigation and testing — Field testing — Part 1: Electrical cone and piezocone penetration test.

[31] Palacky, G. J. (1987). Resistivity characteristics of geologic targets. *Methods in Applied Geophysics Theory, 1, 53-129.*

[32] Robertson, P.K., Campanella, R-G., Gillespie, D.. & Grieg. J. (1986). Use of piezometer cone data. *Proceedings, In-situ '86. AXE Specialty Conference, Blacksburg, VA.*

[33] NF P (1995) Sols : reconnaissance et essais - Détermination des limites d'Atterberg - Partie 1 : limite de liquidité - Méthode du cône de pénétration.NF P94-052-1.

[34] Flavigny E., Desrues J., & Palayer B. (1990). Note technique: le sable d'Hostun «RF». *Revue française de géotechnique, (53), 67-70.*

[35] Apel, H., Thieken, A. H., Merz, B., & Blöschl, G. (2004). Flood risk assessment and associated uncertainty. *Natural Hazards and Earth System Science, 4(2), 295-308.*